Chemical Engineering Journal 161 (2010) 285–288

Contents lists available at ScienceDirect

Chemical Engineering Journal

journal homepage: www.elsevier.com/locate/cej

Photocatalytic activity of Au-buffered WO_3 thin films prepared by RF magnetron sputtering

Hyun Wook Choi [a], Eui Jung Kim [b], Sung Hong Hahn [a,*]

[a] Department of Physics, University of Ulsan, Daehak-ro 102, Nam-gu, Ulsan 680-749, South Korea
[b] Department of Chemical Engineering, University of Ulsan, Ulsan 680-749, South Korea

ARTICLE INFO

Article history:
Received 16 September 2009
Received in revised form 12 January 2010
Accepted 25 January 2010

Keywords:
RF magnetron sputtering
Tungsten oxide thin film
Photocatalytic activity
Visible light

ABSTRACT

Au-buffered WO_3 thin films were deposited on quartz glass using a radio-frequency magnetron sputtering method and their optical, structural and photocatalytic properties were investigated. The photocatalytic activity of the prepared thin films was evaluated by measuring the photodecomposition of methylene blue. The presence of the Au buffer layer improved photodegradation efficiency by about 50%, red-shifted the absorption edge to a longer wavelength, and increased the film surface roughness. Photoexcited charges were separated by surface plasmon resonance at Au nanoparticles.

1. Introduction

Photocatalytic technology has much potential as green energy technology that can be applied to numerous fields [1]. Until now, strenuous efforts to improve the efficiency of photodegradation under a sunlight or indoor light have been made. There are various materials that have the photocatalytic function such as TiO_2, SnO_2, WO_3, ZnO, Fe_2O_3, $FeTiO_3$, CdS, Bi_2O_3 and ZnS [2–10]. Among them, TiO_2 is known to have an excellent ability to purify organic or inorganic pollutants. It has been widely used in the industry due to its chemical stability, harmlessness, inodorous, low cost and abundance [11–13]. Jung et al. has recently reported that Au-doped TiO_2 has an excellent photocatalytic activity [14]. Since TiO_2 has a wide band gap energy (~3.2 eV) [15,16], the photodegradation can be effective under illumination of ultraviolet (UV) light that is about 5% of sunlight [16,17]. Therefore, it is necessary to develop a material photosensitive to visible light. It is well-known that tungsten oxide (WO_3) is stable in acid and that it is photosensitive to visible light because it is an n-type semiconductor material with a band gap energy of 2.5 eV [18–20]. WO_3 has been extensively applied to many fields such as electrochromic devices, smart windows, gas sensors, organic/inorganic hybrid memory devices and solar energy conversion [16,21–24]. But its photocatalytic efficiency is not still satisfactory as the photocarriers generated in the WO_3 conduction band are rapidly recombined [16,24]. Recently, several studies on improving the photodegradation efficiency of WO_3 have been carried out through the doping of transition metals such as Pt, V and Cu or compositing of impurities [4,15,25].

In this study, we have prepared Au-buffered WO_3 thin films by the radio-frequency (RF) magnetron sputtering method. The optical and structural properties of the prepared films were characterized by X-ray diffraction (XRD), scanning electron microscopy (SEM) and scanning probe microscopy (SPM). The photocatalytic activity of the thin films was analyzed by measuring the degradation of methylene blue under irradiation of visible light from a fluorescent lamp.

2. Experimental

Au-buffered WO_3 thin films were deposited on quartz glass by the RF magnetron sputtering method. The WO_3/Au/WO_3 structure was introduced in this work because it is difficult to directly deposit an Au layer on quartz [14]. The RF magnetron sputtering process is a suitable route for the production of high-quality Au-buffered WO_3 thin films. The WO_3 and Au targets with a size of 5×10^{-2} m in diameter were powered by an RF generated at a frequency of 13.56 MHz. The base pressure of the chamber was 3.6×10^{-6} Torr and the deposition pressure was set at 1.0×10^{-2} Torr. The flow rate of Ar (99.99%) was controlled with a mass flow meter system. The optimum substrate-to-target distance was determined to be 150 mm. Before each run, the targets were pre-sputtered in Ar for 5 min to clean the surface of the targets. The RF power of the WO_3 and Au targets was 75 and 15 W, respectively. The as-deposited samples were annealed at 500 °C in air for 1 h. The crystal phase of the prepared thin films was determined by XRD

* Corresponding author. Tel.: +82 52 259 2330; fax: +82 52 259 1693.
E-mail address: shhahn@ulsan.ac.kr (S.H. Hahn).

1385-8947/$ – see front matter © 2010 Elsevier B.V. All rights reserved.
doi:10.1016/j.cej.2010.01.050

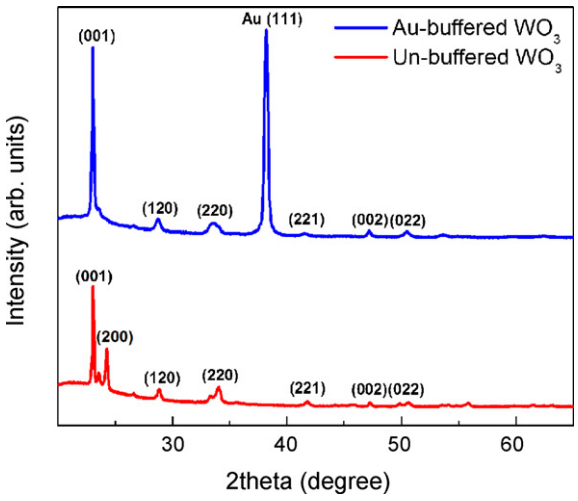

Fig. 1. XRD patterns of un-buffered WO_3 and Au-buffered WO_3 thin films annealed at 500 °C in air for 1 h.

(Philips, X'pert PRO MRD) in the 2θ mode using monochromatic Cu Kα radiation at a grazing incidence. SEM (Carl Zeiss, Supra 40) and SPM (Digital Instruments, Multimode) were employed to investigate the surface morphology of the thin films. The photocatalytic property was evaluated by measuring the photodecomposition of methylene blue ($C_{16}H_{18}ClN_3S$–Cl–$3H_2O$, Sam Chun Pure Chemical Co. LTD.) in water with an initial concentration of 1×10^{-5} mol/L. The samples (2 cm × 2 cm) were immersed in the dye solution in a tubular quartz reactor. The methylene blue solution was vigorously stirred under irradiation of four surrounding 20 W fluorescent lamps (Kumho, FL20SD). Photocatalytic degradation of methylene blue was monitored by measuring the absorbance at 664 nm with a UV–vis spectrophotometer (HP, UV-Vis 8453). The absorbance spectra of the thin films were also measured by the spectrophotometer.

3. Results and discussion

Fig. 1 shows the XRD patterns of WO_3 thin films annealed at 500 °C in air for 1 h. The as-deposited samples were amorphous. The XRD data reveal that the annealed films are crystalline and exhibit the monoclinic structure [12,26]. The monoclinic WO_3 phase is known to be the most stable phase at room temperature [27]. The intensity of the (0 0 1) peak of the Au-buffered WO_3 film was greater than that of the un-buffered WO_3 thin film, and the presence of the Au layer was identified by the large (1 1 1) peak of cubic gold [14]. The crystallite size of the thin films was determined from Scherrer's equation, $D = 0.9\lambda/B\cos\theta$, where D is the crystallite size, λ is the wavelength of X-ray radiation (λ = 1.54056 Å), B is the full width at half-maximum (FWHM), and θ is the half diffraction angle of the cancroids of peak in degree. The crystallite size of the un-buffered and Au-buffered WO_3 thin films was 61.2 and 49.2 nm, respectively, which was determined from the (0 0 1) main peak [28], indicating that the Au buffer layer decreased the crystallite size.

Fig. 2 depicts the SEM images of WO_3 thin films. It can be seen from Fig. 2 that the as-deposited films consist of uniform granular grains (Fig. 2(a) and (c)), while the annealed films consist of non-uniform large grains due to the crystal growth in the thermal process (Fig. 2(b) and (d)). The cross-sectional SEM images show the Au thin layer with a thickness of 10 nm is placed between the top WO_3 layer and bottom WO_3 layer with a thickness of 220 and 40 nm, respectively (Fig. 2(c)).

Fig. 3 illustrates the SPM images of WO_3 thin films. The as-deposited Au-buffered film (Fig. 3(a)) had rougher surface than the as-deposited un-buffered film (Fig. 3(b)). The average surface roughness of the Au-buffered and un-buffered WO_3 films was found to be 0.43 and 0.20 nm, respectively, indicating that the presence of the Au thin layer increases the surface roughness [14]. The annealed Au-buffered film (Fig. 3(b)) had also rougher surface than the annealed un-buffered film (Fig. 3(d)) with an average surface roughness of about 0.88 and 0.72 nm, respectively. Rougher films may provide more reactive surface area, resulting in more photocatalytic activity [29].

Fig. 4 shows the UV–vis absorbance spectra of WO_3 thin films. The absorption edge of the WO_3 thin film was red-shifted in the presence of the Au buffer layer, indicating a reduction of the optical band gap (E_{obg}). The E_{obg} was computed from plots of $(\alpha h\nu)^2 \propto (h\nu - E_g)$, where α is the absorption coefficient and $h\nu$ is the photon energy for the samples. The E_{obg} of the un-buffered and Au-buffered WO_3 thin film was 2.98 eV and 2.88 eV, respectively. A red-shift of the absorption edge of the metal doped WO_3 films is due to the formation of a dopant energy level within the band gap of WO_3. Thus, the optical absorption of the metal doped film depends on the energy levels of the dopant within the WO_3 and the distribution of the dopant metal ions. The Au-buffered WO_3 thin film absorbed the visible light more than the un-buffered WO_3 thin film in the 380–460 nm range. More electrons and holes can be photogenerated in the Au-buffered WO_3 thin films as a result of absorption of more visible light, leading to the enhanced photocatalytic activity.

Fig. 5 shows the photocatalytic degradation of methylene blue for various samples under fluorescent lamp irradiation for 6 h. The photoactivity of the films was found to be in the order: Au-buffered WO_3 film > un-buffered WO_3 film > TiO_2 film > blank. Note the TiO_2

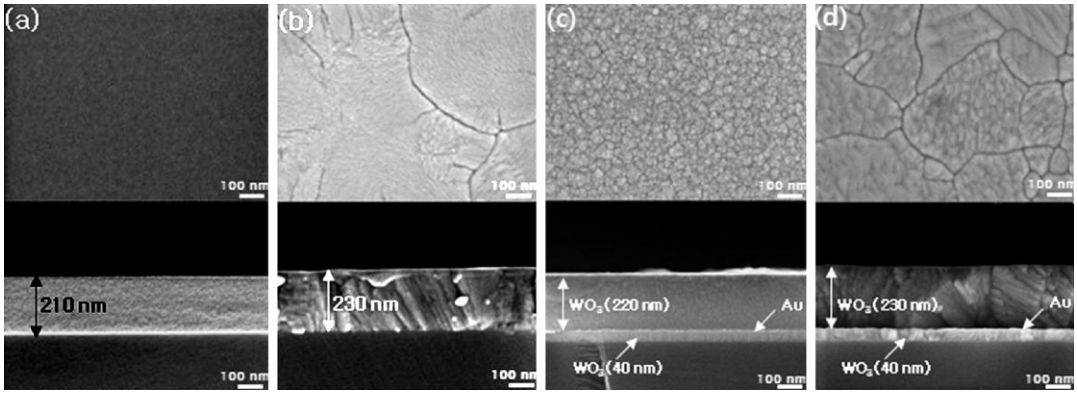

Fig. 2. Surface and cross-sectional SEM images of WO_3 thin films: as-deposited (a), annealed at 500 °C (b) and Au-buffered WO_3 thin films: as-deposited (c), annealed at 500 °C (d).

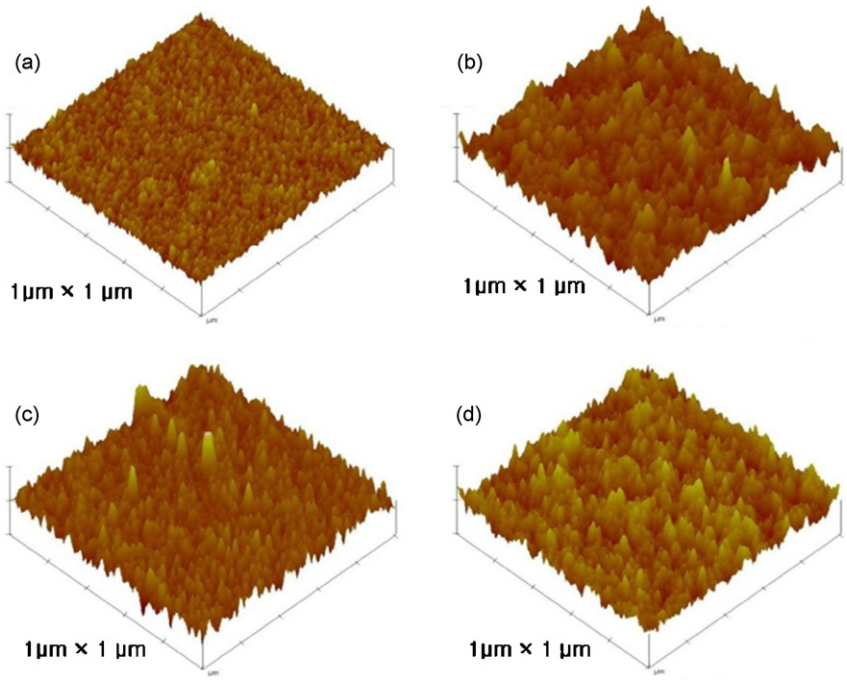

Fig. 3. SPM images of WO_3 thin films: as-deposited (a), annealed at 500 °C (b) and Au-buffered WO_3 thin films: as-deposited (c), annealed at 500 °C (d).

film with 220 nm thickness had negligible photoactivity similar to the blank sample. Furthermore, the photocatalytic efficiency of the Au-buffered WO_3 film was about 50% greater than that of the un-buffered WO_3 thin film. The photocatalytic activity of the WO_3 films turned out to negligibly change after their repeated use. Our results show that WO_3 is an excellent photocatalytic material than TiO_2 in the visible light range and the presence of the Au buffer layer significantly improves the photocatalytic efficiency.

Schematic illustration of the photocatalytic mechanism for the Au-buffered WO_3 thin film is shown in Fig. 6. When the energy higher than the band gap energy of WO_3 is absorbed, electron and hole pairs are generated in WO_3. The photocatalytic activity depends on the number of photogenerated electrons and holes and their recombination life time. The photogenerated holes in the valence band react with the H_2O on the surface of the WO_3 thin film to produce hydroxyl radicals (•OH) that have strong oxidative capability. On the other hand, the photogenerated electrons in the

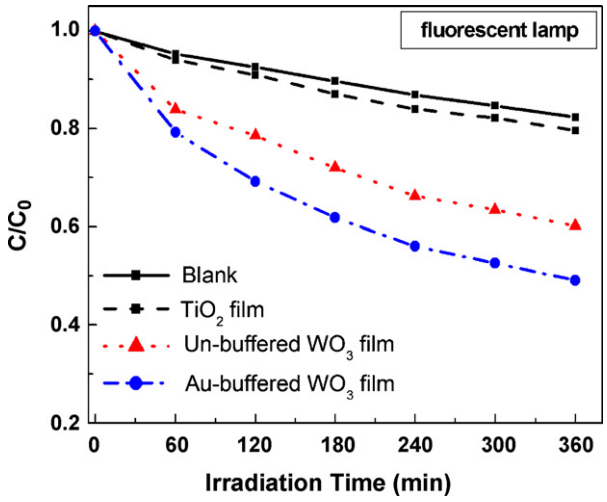

Fig. 5. Photodegradation of methylene blue for un-buffered and Au-buffered WO_3 thin film under fluorescent lamp irradiation.

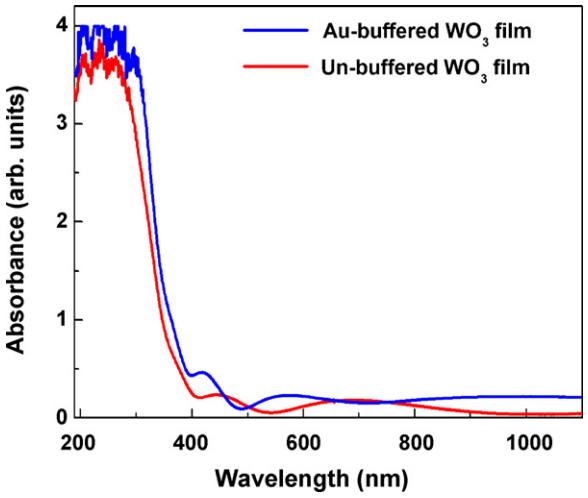

Fig. 4. UV–vis absorbance spectra of un-buffered WO_3 and Au-buffered WO_3 thin films annealed at 500 °C in air for 1 h.

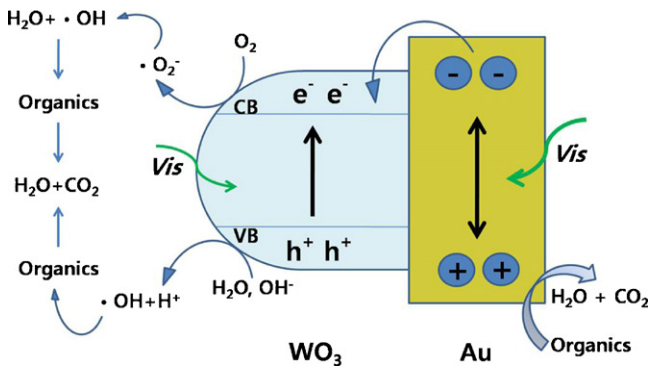

Fig. 6. Schematic illustration of photocatalysis mechanism for Au-buffered WO_3 thin film.

conduction band combine with the oxygen to form $\bullet O_2^-$, which produce the hydroxyl radical by reacting with H_2O. Moreover, the Au-buffered WO_3 thin film utilizing a visible light induces charge separation. When it is irradiated by enough visible light with higher energy than the band gap, Au nanoparticles in the Au-buffered WO_3 thin film are photoexcited. Charges are then separated at the Au–WO_3 interface due to surface plasmon resonance [30,31], as shown in Fig. 6. Electrons generated at the Au particle are moved to the conduction band of WO_3 and contributes to the photocatalytic activity. The holes in the Au particles are also involved in the photocatalytic reaction. As a result, the photocatalytic activity of the Au-buffered WO_3 thin films is greater than the un-buffered WO_3 thin film. The methylene blue molecules might be decomposed to form organic acids as the intermediate products [32].

4. Conclusions

Un-buffered and Au-buffered WO_3 thin films were prepared by the RF sputtering method and their optical, structural, and photocatalytic properties were investigate. XRD results showed that the 500 °C-annealed WO_3 films had the crystalline monoclinic structure and that the presence of the Au buffer layer slightly decreased the crystallite size. The surface roughness of the Au-buffered WO_3 film was much greater than that of the un-buffered film. The absorption edge of the Au-buffered film was red-shifted to a longer wavelength compared to the un-buffered film. The Au-buffered WO_3 film absorbed visible light more than the un-buffered WO_3 film in the 380–460 nm range. The photoactivity of the Au-buffered WO_3 film was about 50% greater than that of the un-buffered WO_3 film.

Acknowledgement

This work was supported by the 2008 Research Fund of the University of Ulsan.

References

[1] C.C. Chan, C.C. Chang, W.C. Hsu, S.K. Wang, J. Lin, Photocatalytic activities of Pd-loaded mesoporous TiO_2 thin films, Chem. Eng. J. 152 (2009) 492–497.
[2] L. Wei, C. Shifu, Z. Wei, Z. Sujuan, Titanium dioxide mediated photocatalytic degradation of methamidophos in aqueous phase, J. Hazard. Mater. 164 (2009) 154–160.
[3] L.C. Chen, F.R. Tsai, S.H. Fang, Y.C. Ho, Properties of sol–gel SnO_2/TiO_2 electrodes and their photoelectrocatalytic activities under UV and visible light illumination, Electrochim. Acta 54 (2009) 1304–1311.
[4] Y.H. Kim, H. Irie, K. Hashimoto, A visible light-sensitive tungsten carbide/tungsten trioxide composite photocatalyst, Appl. Phys. Lett. 92 (2008) 182107.
[5] C. Shifu, Z. Wei, Z. Sujuan, L. Wei, Preparation, characterization and photocatalytic activity of N-containing ZnO powder, Chem. Eng. J. 148 (2009) 263–269.
[6] W. Zhou, W. He, J. Ma, M. Wang, X. Zhang, S. Yan, X. Tian, X. Sun, X. Han, Biosynthesis of mesoporous organic–inorganic hybrid Fe_2O_3 with high photocatalytic activity, Mater. Sci. Eng. C 29 (2009) 1893–1896.
[7] B. Gao, Y.J. Kim, A.K. Chakraborty, W.I. Lee, Efficient decomposition of organic compounds with $FeTiO_3$/TiO_2 heterojunction under visible light irradiation, Appl. Catal., B: Environ. 83 (2008) 202–207.
[8] M.A. Zhukovskiya, A.L. Stroyukb, V.V. Shvalaginb, N.P. Smirnovaa, O.S. Lytvync, A.M. Eremenko, Photocatalytic growth of CdS, PbS, and Cu_xS nanoparticles on the nanocrystalline TiO_2 films, J. Photochem. Photobiol. A 203 (2009) 137–144.
[9] S.Y. Chai, Y.J. Kim, M.H. Jung, A.K. Chakraborty, D.W. Jung, W.I. Lee, Heterojunctioned $BiOCl$/Bi_2O_3, a new visible light photocatalyst, J. Catal. 262 (2009) 144–149.
[10] A. Deshpande, P. Shah, R.S. Gholap, N.M. Gupta, Interfacial and physicochemical properties of polymer-supported CdS·ZnS nanocomposites and their role in the visible-light mediated photocatalytic splitting of water, J. Colloid Interface Sci. 333 (2009) 263–268.
[11] A. Fujishima, T.N. Rao, D.A. Tryk, Titanium dioxide photocatalysis, J. Photochem. Photobiol. C 1 (2000) 1–21.
[12] H. Liu, T. Peng, D. Ke, Z. Peng, C. Yan, Preparation and photocatalytic activity of dysprosium doped tungsten trioxide nanoparticles, Mater. Chem. Phys. 104 (2007) 377–383.
[13] S. Sakthivel, M.V. Shankar, M. Palanichamy, B. Arabindoo, D.W. Bahnemann, V. Murugesan, Enhancement of photocatalytic activity by metal deposition: characterization and photonic efficiency of Pt, Au and Pd deposited on TiO_2 catalyst, Water Res. 38 (2004) 3001–3008.
[14] J.M. Jung, M. Wang, E.J. Kim, C. Park, S.H. Hahn, Enhanced photocatalytic activity of Au-buffered TiO_2 thin films prepared by radio frequency magnetron sputtering, Appl. Catal. B: Environ. 84 (2008) 389–392.
[15] X.Z. Li, F.B. Li, C.L. Yang, W.K. Ge, Photocatalytic activity of WO_x–TiO_2 under visible light irradiation, Photochem. Photobiol. A 141 (2001) 209–217.
[16] X.F. Cheng, W.H. Leng, D.P. Liu, J.Q. Zhang, C.N. Cao, Enhanced photoelectrocatalytic performance of Zn-doped WO_3 photocatalysts for nitrite ions degradation under visible light, Chemosphere 68 (2007) 1976–1984.
[17] F. Kojin, M. Mori, Y. Noda, M. Inagaki, Preparation of carbon-coated $W_{18}O_{49}$ and its photoactivity under visible light, Appl. Catal. B: Environ. 78 (2008) 202–209.
[18] M.S. Ulmann, J. Augustynski, Aging effects in *n*-type semiconducting WO_3 films, J. Appl. Phys. 54 (1983) 6061–6064.
[19] B. Marsen, E.L. Miller, D. Paluselli, R.E. Rocheleau, Progress in sputtered tungsten trioxide for photoelectrode applications, Int. J. Hydrogen Energy 32 (2007) 3110–3115.
[20] T.G.G. Maffeis, D. Yung, L. LePennec, M.W. Penny, R.J. Cobley, E. Comini, G. Sberveglieri, S.P. Wilks, STM and XPS characterization of vacuum annealed nanocrystalline WO_3 films, Surf. Sci. 601 (2007) 4953–4957.
[21] A.A. Joraid, Comparison of electrochromic amorphous and crystalline electron beam deposited WO_3 thin films, Curr. Appl. Phys. 9 (2009) 73–79.
[22] S.R. Bathe, P.S. Patil, Titanium doping effects in electrochromic pulsed spray pyrolyzed WO_3 thin films, Solid State Ionics 179 (2008) 314–323.
[23] A. Subrahmanyam, A. Karuppasamy, Optical and electrochromic properties of oxygen sputtered tungsten oxide (WO_3) thin films, Solar Energy Mater. Solar Cells 91 (2007) 266–274.
[24] K.M. Karuppasamy, A. Subrahmanyam, The electrochromic and photocatalytic properties of electron beam evaporated vanadium-doped tungsten oxide thin films, Solar Energy Mater. Solar Cells 92 (2008) 1322–1326.
[25] H. Irie, S. Miura, K. Kamiya, K. Hashimoto, Efficient visible light-sensitive photocatalysts: grafting Cu(II) ions onto TiO_2 and WO_3 photocatalysts, Chem. Phys. Lett. 457 (2008) 202–205.
[26] J. Rajeswari, B. Viswanathan, T.K. Varadarajan, Tungsten trioxide nanorods as supports for platinum in methanol oxidation, Mater. Chem. Phys. 106 (2007) 168–174.
[27] G.R. Bamwenda, H. Arakawa, The visible light induced photocatalytic activity of tungsten trioxide powders, Appl. Catal. A: Gen. 210 (2001) 181–191.
[28] W.S. Choi, E.J. Kim, S.G. Seong, Y.S. Kim, C.H. Park, S.H. Hahn, Optical and structural properties of ZnO/TiO_2/ZnO multi-layers prepared via electron beam evaporation, Vacuum 83 (2009) 878–882.
[29] J.M. Valtierra, C.F. Reyes, J.R. Ortıïz, E. Moctezuma, F. Ruiz, Preparation of rough anatase films and the evaluation of their photocatalytic efficiencies, Appl. Catal. B: Environ. 76 (2007) 264–274.
[30] Y. Tian, T. Tatsuma, Mechanisms and applications of plasmon-induced charge separation at TiO_2 films loaded with gold nanoparticles, J. Am. Chem. Soc. 127 (2005) 7632–7637.
[31] Y. Takahashi, T. Tatsuma, Visible light-induced photocatalysts with reductive energy storage abilities, Electrochem. Commun. 10 (2008) 1404–1407.
[32] C.-H. Wu, J.-M. Chern, Kinetics of photocatalytic decomposition of methylene blue, Ind. Eng. Chem. Res. 45 (2006) 6450–6457.